59th ILMENAU SCIENTIFIC COLLOQUIUM
Technische Universität Ilmenau, 11 – 15 September 2017
URN: urn:nbn:de:gbv:ilm1-2017iwk-138:9

PHOTOMETRIC DATA FOR THE DEVELOPMENT OF LIGHTING COMPONENTS

Knut Bredemeier

TechnoTeam Bildverarbeitung GmbH – www.technoteam.de

ABSTRACT

The availability of accurate photometric data is crucial for the development of lighting technology components. Especially in the course of the displacement of the classical lamps by solid-state lighting (SSL) technologies and the resulting increased range of lighting applications, the requirements for these measurement data have increased. Here, optical simulation programs based on ray tracing algorithms (Computer-Aided Lighting – CAL) open up new development processes.

State-of-the-art is the use of ray files measured by camera-based near-field goniophotometers. Some of those systems also offer measurements of the luminous intensity distribution, luminous flux and goniospectrometric data in conformity with IES LM-79-08, EN 13032-4 and CIE S 025, and can thus also take over the classical measurement tasks of far-field goniophotometers.

This paper illustrates applications of the data measured with near-field goniophotometers and luminance measuring cameras in the field of simulation, glare evaluation and luminaire characterization.

Index Terms - photometric data, lighting technology, solid-state lighting - SSL, goniophotometer, ray files. near-field photometry, imaging luminance measuring device - ILMD

1. LIGHTING COMPONENTS

The chosen term “lighting components” is of a very general nature and relates to light sources, to elements involved in the light guidance, and to complete systems. As for the lighting systems, a fundamental classification into systems for illumination purposes and signal or also display lighting can be made. The function of illumination systems such as luminaires, floodlights or headlamps is to ensure in an efficient way the application-specific distribution of the light emitted by the source(s). In the case of signal or display lighting systems (rear lights, back-lit symbols or display elements), however, the main purpose is to ensure the good visibility, which often puts the evaluation of the luminance distribution in the foreground.

2. LUMINANCE MEASUREMENT

For a wide range of conditions the luminance corresponds to the impression of the brightness the human eye gets. Thus, it is the photometric quantity which is directly linked to the sensory perception. Therefore, image-resolved luminance measurement data are used in many cases in the development and evaluation of lighting components. Imaging luminance measuring cameras (ILMD) can be employed as stand-alone measuring systems or are a component part

of, for example, a near-field goniophotometer (cf. paragraph 4). In the following figures, various applications are shown.

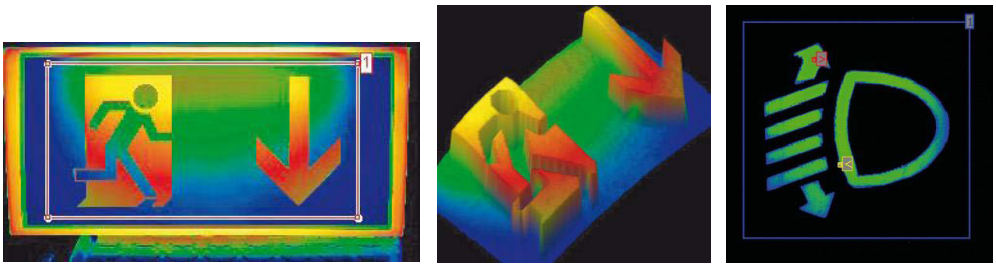

Figure 1: Evaluation of emergency lights and backlit symbols (night vision design)

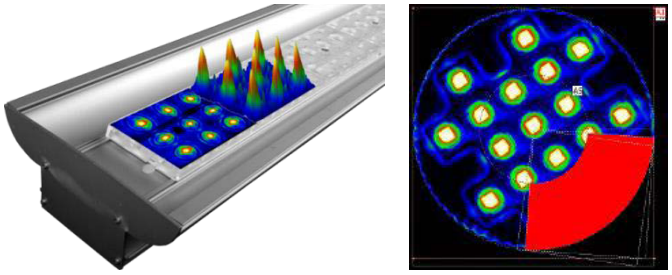

Figure 2: Left: Luminance distribution of luminaires (e.g. for glare evaluation), right: Luminance evaluation of LED modules (e.g. according to Zhaga)

3. RAY DATA AND LUMINOUS INTENSITY DISTRIBUTIONS FOR THE DEVELOPMENT PROCESS

The ever shorter development cycles of lighting components place high demands on the development process of complete lighting systems. The number of iterations of design, prototype construction and validation shall be as low as possible, which can only be achieved through a realistic optical design. For this procedure, calculation methods of geometrical optics and, where applicable, also methods of wave optics are applied [1]. Since the nineties, a number of high-performance software tools based on ray-tracing algorithms have been available for this purpose, which were at first be used e.g. for the development of novel headlamp systems. Anyway, these tools are now being widely used.

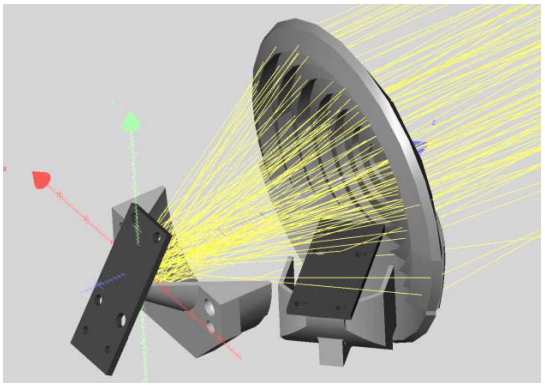

Figure 3: Simulation of a headlamp module

A realistic optical simulation presupposes the knowledge and the algorithmic consideration of the exact optical characteristics of all components involved in light guidance, and of the radiation characteristic of the light source(s). In the case of simple modelling, a luminous

intensity distribution $I_v(\theta, \varphi)$ is used, i.e., a point light source is assumed. On the basis of the photometric inverse square law, the illuminance at a distance of r results in

$$E_v = \frac{I_v}{r^2}.$$

This approach, however, often entails large errors if the spatial expansion of the light source in relation to the distance to the subsequent lighting components is large. For the sake of clarity, Figure 4 shows the difference of the ray path of a point light source (red lines) and a spatially distributed light source (green lines) onto a near Fresnel lens.

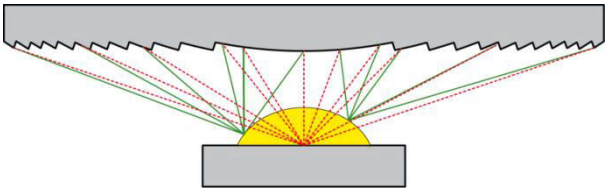

Figure 4: Comparison of a ray path of a point light source and a spatially distributed light source

Thus, it is indispensable to take the spatially distributed radiation characteristic into consideration. Optical simulation programs offer the possibility of applying those synthetic models of the light source which try to recreate the internal structure and the optical material properties. This, however, cannot always be achieved in a satisfactory way, and requires an enormous amount of time, too. Therefore, the metrological approach is often chosen, which means that the radiation characteristic of the light source(s) is measured rather than synthetized.

Since the early nineties, the measurement of the radiation characteristic by means of near-field goniophotometers has been state-of-the-art [2] [3]. These devices use an imaging luminance measuring camera (ILMD) in order to record the complete luminance distribution of a light source and to output these values in the form of so-called ray data. A ray set $\Phi_v(x, y, z, \theta, \varphi)$ consists of a very large number of vectors (10^6…10^9) with luminous flux amounts, and can be used by all conventional optical simulation programs. Figure 5 shows the LID (3D representation) and the ray data of a laterally emitting LED.

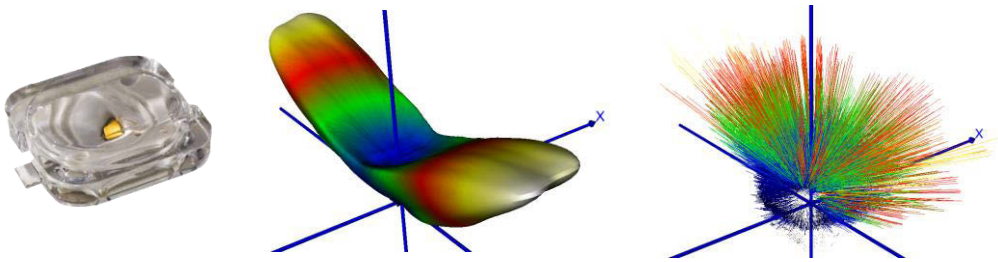

Figure 5: LED, luminous intensity distribution (3D representation), ray data

If the luminous flux portion is calculated from the ray data onto a surface elements, the illuminance results to:

$$E_v = \frac{d\Phi_v}{dA}.$$

As an example, the illuminance distribution of the LED from Figure 5 has been calculated on a plane 10 mm above it first with the LID, and then with the ray data. Figure 6 shows both distributions with relative scaling. As was to be expected, clear differences can be seen due to the short distance.

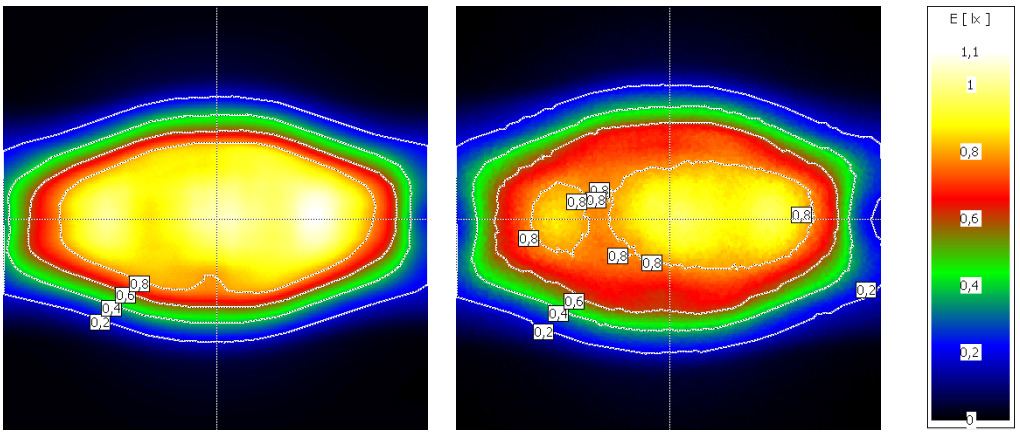

Figure 6: Illuminance distribution (relative) on a plane 10 mm above, calculation carried out with LID (left) and with ray data (right)

On the basis of the horizontal and the vertical cross-sectional profiles (Figure 7), deviations in a range up to 10 % can be found. At a distance of the plane of 50 mm, the differences for these LEDs are already negligible so that calculation could be made with the LID.

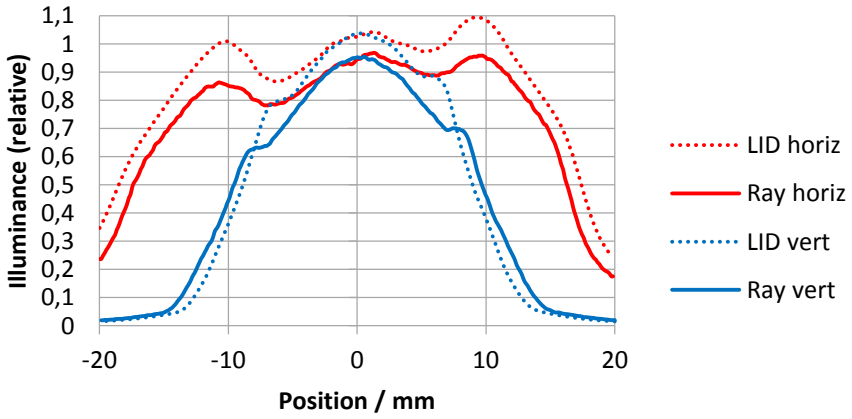

Figure 7: Horizontal and vertical cross-sectional profiles of the illumination intensity distributions (LID and ray data)

Some applications require the calculation of the illuminance distribution on a surface close to a luminaire [4]. Here only the usage of measured ray files is the only way for getting correct results.

4. MEASUREMENT AND PROPERTIES OF RAY DATA

An optics designer without an own goniophotometer for ray data measurement will use either already prepared ray files available in a suitable file format and with a well-defined number of rays, or a manufacturer-specific format with suitable conversion program. In order to be able to better evaluate the properties, boundary conditions, application limitations and uncertainties of the data, some aspects are explained in more detail below.

4.1 Measuring principle

The radiation characteristic of a light source can be described in a general way using the 7D plenoptic function [5].

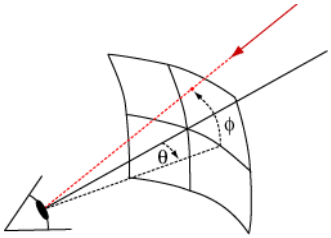

$$P = P(\theta, \phi, \lambda, t, V_x, V_y, V_z)$$

This function contains virtual viewing positions V_x, V_y, V_z with the corresponding directions θ, ϕ. With λ, the spectral properties are taken into account, and, furthermore, with t the function is time-variant.

A metrological determination of this function can only be achieved by reducing the dimension. If a static condition is presupposed, t becomes void. The spectral properties are determined as integral portions, for example by a photometric evaluation with the luminosity function $V(\lambda)$ or as color channels (cf. paragraph 4.3). Then, the 5D plenoptic function results, which is also called *Light field* [6].

$$P = P(\theta, \phi, V_x, V_y, V_z)$$

A metrological determination of this vector function is only possible through discretization and results in the ray set

$$\Phi_v(x, y, z, \theta, \varphi)$$

The near-field goniophotometers commercially available for the measurement of ray data rely on the same basic measuring principle but the concrete application is greatly manufacturer-specific. In this paper, only the measuring principle of the goniophotometers type TechnoTeam RiGO801 [7] can briefly be described. RiGO801 stands for a model series of goniophotometers for various maximum dimensions of the devices under test (DUT). The smallest system with a maximum DUT of 200 mm is designed for LEDs/OLEDs measurements and the larger types are able to measure any kind of lighting products up to a dimension of 2000 mm.

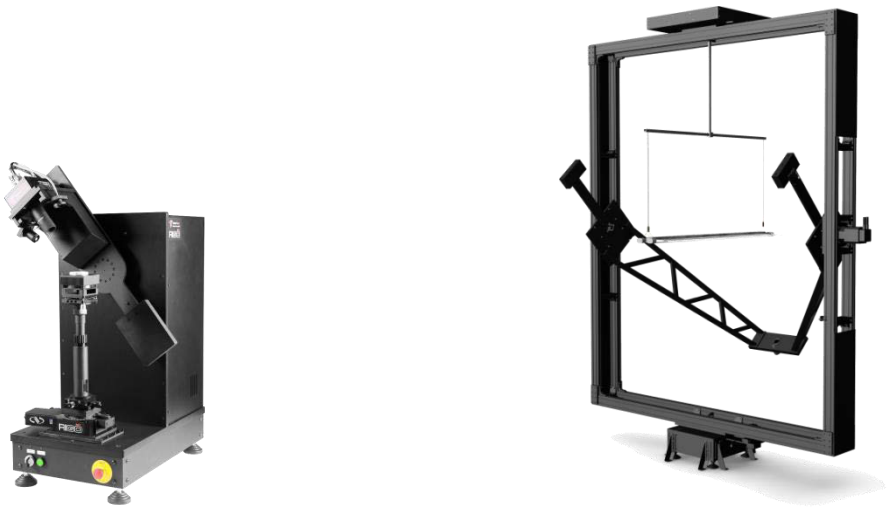

Figure 8: Goniophotometer type RiGO801 – LED (left), RiGO801 – 2000 (right)

In the case of the RiGO801 goniophotometers, an imaging luminance measuring device type LMK-5 [8] is moved around the DUT at a constant distance. In doing so, luminance images are being measured “on-the-fly” in a selectable angular grid.

Using the calibration data of the lens employed, the pixel coordinates can be converted to vectors in the camera coordinate system (Figure 9), and finally transformed into the world coordinate system of the goniometer with the camera position. Thus, the “rays” are defined.

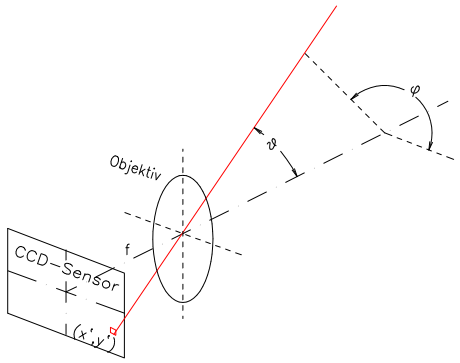

Figure 9: Camera coordinate system

By means of the geometrical calibration data, the luminances of the images are calculated to luminous flux portions, which correspond to the vector magnitudes (Figure 10).

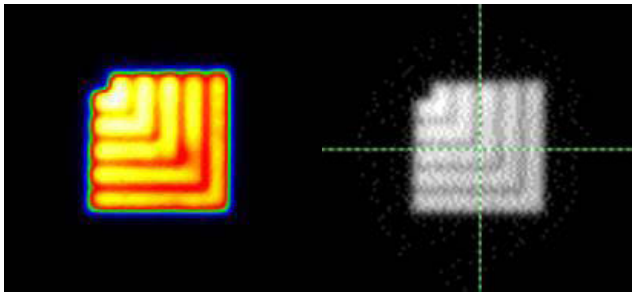

Figure 10: Luminance image (left) and corresponding luminous flux portions (right)

For an efficient storage of the data in the TTR file format, it is not the transformed ray data which are saved, but the images of the luminous flux portions instead, which can easily be compressed due to the regular pixel grid (see Figure 11). By means of the geometrical calibration data, the ray transformation can be carried out later. For this, a conversion program without license fees – *Converter801* – is available [9] which allows the ray data to be converted into all common file formats.

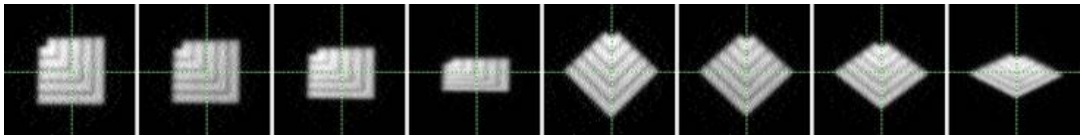

Figure 11: Sequence of images with luminous flux portions in a TTR file

For evaluating and applying the measured ray data, the exact knowledge of the position of the coordinate system to the DUT is important. Therefore, before measurement starts, some pictures are taken by the camera from different perspectives, with external illumination being switched on, and the coordinate system displayed (see Figure 12).

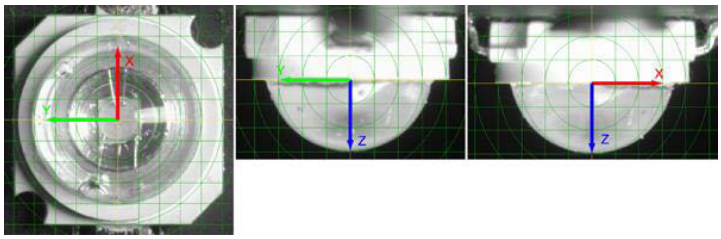

Figure 12: Position of the coordinate system relative to the DUT

4.2 Calculation of the luminous intensity distribution from ray data

The information of the luminous intensity distribution can be derived from the complex emission characteristic of a ray set. The luminous intensity is the luminous flux per solid angle.

$$\mathrm{I}_v(\theta,\varphi) = \frac{\Delta\Phi_v(\theta,\varphi)}{\Delta\Omega(\theta,\varphi)}$$

The ray data contain the luminous flux portions in all directions, i.e., for calculating luminous intensities from ray data, the luminous flux portions only have to be added up into the corresponding solid angles. Thus, also the luminous intensity distribution can be measured by measuring the ray data by means of a near-field goniophotometer.

4.3 Spectral ray data

So far, only photometric ray data with luminous flux amounts have been considered. In order to take wavelength-dependent refraction (dispersion) into account, however, the spectral distribution of the ray data is important, i.e., each ray should contain the spectral power distribution. Anyway, this is not realizable neither from a metrological point of view nor as far as the amount of data is concerned. Therefore, alternatively multi-channel measurements are made, for example by using spectral filter glasses.

In the case of phosphor-converted white LEDs, the separation of the blue from the yellow spectral parts using suitable filters is generally applied [10]. The wavelengths of the ray data are calculated according to these distributions, which allows dispersive components to be simulated in a more realistic way.

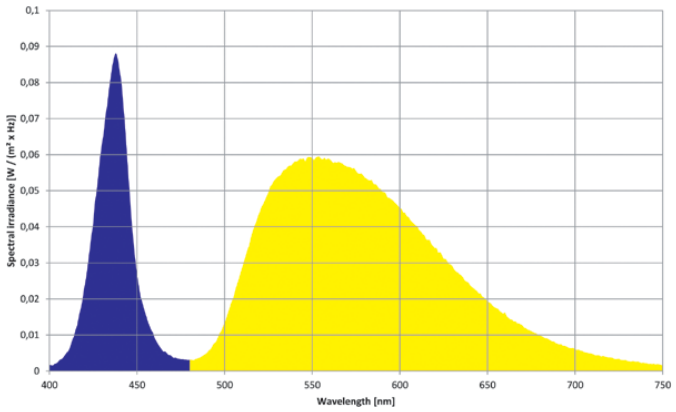

Figure 13: Separation into the blue and yellow spectral range

In the case of complex spectral distributions, this method, however, has its limits, i.e., the type of filters and number of channels used must be adapted if necessary [11].

4.4 File formats

The measuring programs of the goniophotometers output the ray data in general in a manufacturer-specific file format which must be converted into a format that can be read by the simulation program used. Before the file format IES TM-25 [12] was introduced in 2013, the programs had specified their own file formats (e.g. ASAP®, SPEOS™, Light Tools®, Zemax®, TracePro®, …), which were nearly identical. However, when spectral information was to be supported, they partly presented some restrictions. Meanwhile, the TM-25 format is widely supported, which greatly facilitates the provision of the ray data.

4.5 Measurement uncertainties, resolution and dynamic range

A ray set is the discretized vector function of a light field (cf. paragraph 4.1). Due to the complexity of the measuring quantity and the measuring technique, the complete description of the measurement uncertainties of ray data has been an unsolved problem so far. There are no procedures for comparing two ray sets directly. A comparison or evaluation is made in general via derived quantities such as the luminous intensity distribution [13] or illuminances.

Therefore, as user of ray data, the question arises of the "quality" of the available data. In the following, some fundamental aspects shall be discussed.

4.5.1 Uncertainties of the rays

The rays have starting points, directions and magnitudes (luminous flux), all of which present measurement uncertainties. The starting points and directions are influenced by the following factors:

- accuracy of the goniometer coordinate system, i.e., intersection of the axes and orthogonality
- intersection of the optical axis of the camera with the center of the goniometer coordinate system from all directions
- accuracy of the camera model (lens distortion, influences exerted by filters)
- absolute precision of the camera positions (distance, angle)

The accuracy of the luminous flux amounts is mainly influenced by:

- the accuracy of the luminance measurement
- the precision of the solid angles (pixels) necessary for transforming luminances into luminous flux portions

On the basis of the ray data, some essential quality features can possibly be derived. By simulating the luminance distribution in the plane of the light source with a sufficiently high number of rays, the sharpness of the possibly existing structures can be checked. Fuzzy structures indicate position tolerances of the rays on the plane. Also, the position of the light source can be checked from different lateral directions by making simulations on planes in the center of the coordinate system. The transformation of the ray data into the luminous intensity distribution, and a comparison with potentially available reference data represent a possibility of evaluating the overall distribution.

4.5.2 Measurement resolution

As already explained, a vector function is discretized when measuring ray data. Generally, the discretization of a signal profile requires to stick to the Nyquist-Shannon sampling theorem [14]. Thinking of a frequency signal, the sampling must take place with at least the double sampling frequency of the maximum frequency component contained, otherwise aliasing

effects will turn up. To prevent those effects from turning up, too high frequency components are usually filtered out of the signal before discretization (analog low pass filter).

Applied to ray data, sampling is multidimensional and considerably more complex here [15] and also analog low pass filtering is no option. Both the camera image and the camera positions are discretized. It is no longer easy to determine the optimum sampling step widths (pixels, angles), so two criteria must be considered here, the gradients in the luminous intensity distribution and the optical flow [16] of the luminance images.

It seems plausible that the angular step widths must be sufficiently small in order to sample the gradients of the luminous intensity distribution finely enough. Figure 14 shows two luminous intensity distribution curves of LEDs with lenses which present very high gradients and complex distributions. Both measurements were made at 0.75° x 0.75° as a larger step width would greatly falsify the distributions.

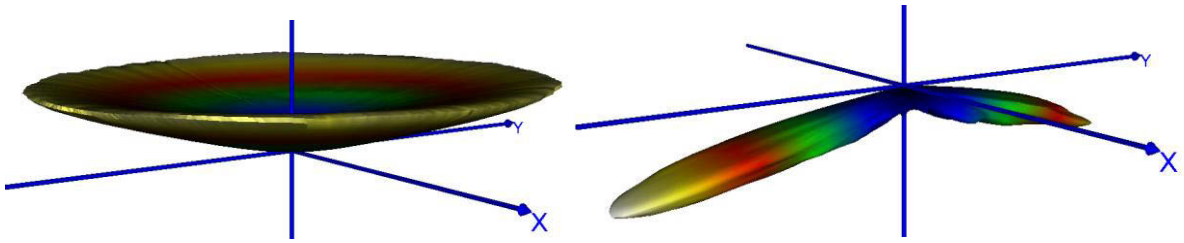

Figure 14: LIDs with high gradients (LEDs with lenses)

On the other hand, the criterion of the change of the luminance distributions of the measurement positions (optical flow) cannot be evaluated easily. The luminance images are captured only at discrete angular positions so that the image information changes more or less strongly from image to image, depending on the DUT. Thus, the measuring algorithms of the near-field goniophotometers must interpolate the luminance distributions between the images, which is always subject to errors. In the case of LEDs with lambert-shaped luminous intensity distribution, a large step width could be chosen (e.g. 5° x 5°) from the point of view of the small gradients prevailing here. Anyway, what about the change of the luminance distribution in the near field? For example, the near-field distribution of multi-chip LEDs or LEDs with lenses could be more complex, and particularly this near-field characteristic shall exactly be contained in the ray data. Therefore, it is advisable to generally use a high angular resolution.

4.5.3 DUT orientation and manufacturing tolerances

A near-field goniophotometer measures the ray data of a light source in the goniometer coordinate system. When preparing the measurement, the DUT is positioned such that the relation of the object coordinate system to the device coordinate system can easily be determined by means of camera images (cf. Figure 12). For this, some unambiguous characteristics such as the edges of the housing or the position of an LED chip or lens can be used as reference points. This assignment presents some uncertainties in the position and tilt angles which are mainly influenced by:

- restricted visibility of edges or structures through fuzzy imaging (depth of field od the lens)
- selection of a suitable illumination (incident light or/and backlighting)
- visibility of lens contours

Another aspect relates to taking manufacturing tolerances of the DUT into account. In the case of LEDs, there are tolerances of the position of the LED chips and lenses in relation to

the reference layout described in the data sheet, and certainly also scattering of other properties. Has a particularly “good” DUT been chosen for the measurement?

4.6 Starting coordinates and geometry of the light source

The measuring cameras of the goniophotometers can only supply directional information but no depth information, i.e., the real starting coordinates of the rays emitted by the light source are unknown. For the simulation, however, it is necessary to know the starting points of the vectors, which are usually calculated using ray-tracing algorithms onto a virtual enveloping surface (target geometry). The enveloping surface can be a simple basic geometry (sphere, cuboid, cylinder), complex 3D-CAD models of the DUT or even unknown distributions.

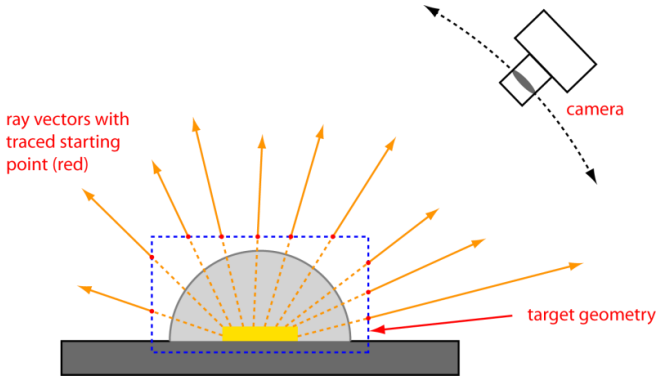

Figure 15: Tracing of ray vector starting points to a target geometry

When choosing the enveloping geometry of the DUT used for raytracing, it has to be ensured that all relevant light-emitting regions are included. Due to the tolerances in assigning the position of the coordinate system relative to the DUT, and due to the geometrical measurement uncertainties of the ray data, a slightly larger target geometry should be chosen. (cf. paragraph 4.7). Otherwise, it can be that not all regions are included. Thus, caution is required when using the ideal 3D-CAD data.

Now, the starting points of the rays are positioned on the surface of the target geometry, which has a well-defined “safety distance” to the light source. If there are some optical elements near the light source during simulation, undercuts with the target geometry may result, and the starting points in the regions concerned lie within these elements. In this case, simulation is faulty unless it is treated separately. During the ray generation on the basis of RiGO801 measurement data, a so-called volume mode is available as an alternative for calculating the starting points onto the surface of the target geometry. In this mode, the starting points are positioned, in each case, onto the center between the two intersection points of a ray vector with the geometry. Thus, the starting points are concentrated within the geometry.

As an example, the evaluation of the distribution of the starting points of the rays on the basis of an online available ray set of a 4-chip LED made by a well-known LED manufacturer is described in the following. According to the data sheet, the coordinate center of the ray data is in centered to the 4 LED Chips (cf. Figure 16), and no information at all is given on the distribution of the starting points.

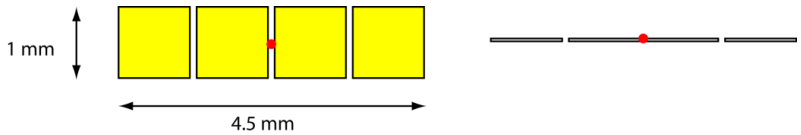

Figure 16: Position of the coordinate center (top view – left, lateral view – right)

For analyzing the distribution of the starting points, the luminous flux amounts of the rays were projected in two planes for top view and lateral view (Figure 17). The lateral view reveals an interesting distribution showing that the starting points are positioned up to 0.8 mm above the LED plane. If required, this should be taken into consideration when using the data for an optics simulation.

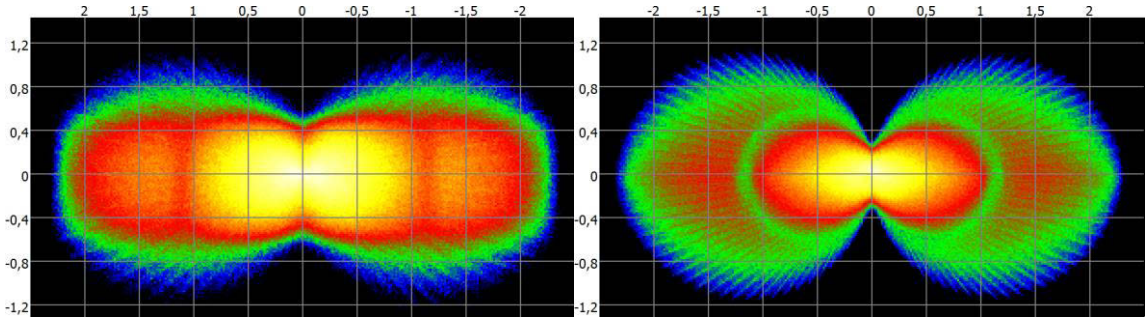

Figure 17: Projection of the starting points of the rays for top view (left-hand side) and lateral view (right-hand side), axis scaling in mm, luminous fluxes in false-color representation and logarithmically scaled

4.7 Elements captured and radiation range of the DUT

Without any additional information on the ray set, it is not possible to recognize which angular range has exactly been captured or also if the entire radiation characteristic of the light source is contained. Many LEDs also emit significant portions into ranges larger than +/- 90°, which raises the question of how the LED was operated for the measurement or also how it was fixed. In this case, an LED board or a test fixture shades those portions which are possibly relevant to a simulation.

There are examples which show that the LED board is regarded as optical unit with the LED and provided, for example, with certain reflection characteristics. In this case, however, the board must be considered to be part of the measurement, and, thus, the field of view of the camera must be sufficiently large. Otherwise, the LED must be mounted in a way as to allow the entire radiation area to be captured, and the board to be correctly taken into account in the simulation. When choosing the target geometry, the board must also be included as part of the light source. Another possibility is to choose deliberately a smaller geometry in order to eliminate those portions and to evaluate them separately, if necessary.

Figure 18 (left-hand side) shows an example of the luminance profile of an LED with PCB along a cut.

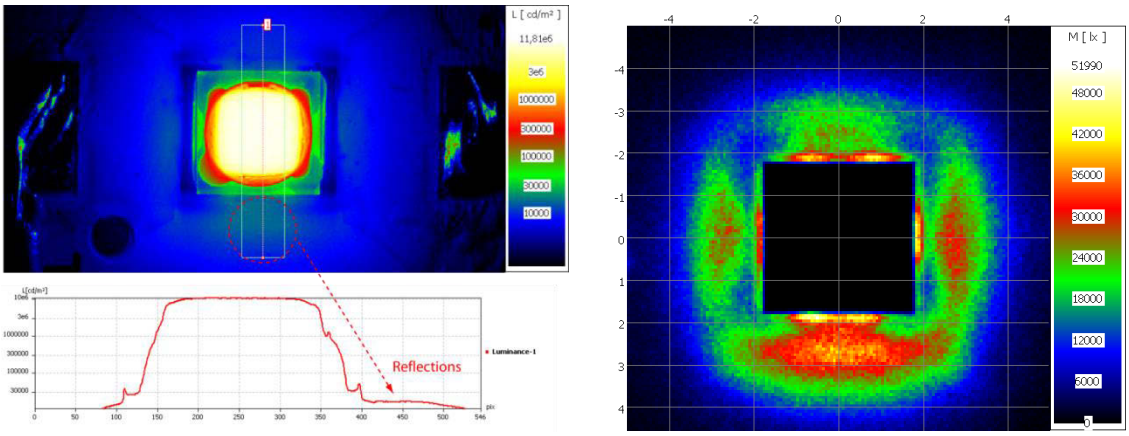

Figure 18: Luminance profile of an LED with board (logarithmic scaling) and luminous emittance distribution M(x',y') emitted by PCB

The luminance portions of the PCB are clearly visible. For analyzing the ray data generated in this region, a target geometry was chosen which only captures the LED, and then calculates the illuminance distribution or, to be more exact, the specific light emission on the board (Figure 18 – right-hand side). In this example, the portion corresponds to 1.3 % of the total luminous flux.

5. MEASUREMENT OF THE LUMINOUS INTENSITY DISTRIBUTION

When developing luminaires, the measurement of the luminous intensity distribution of prototypes and of the final product is indispensable. In the following, some common measuring procedures and systems are described.

5.1 Far-field measurement via the illumination intensity

The far-field measurement of the luminous intensity is based on the photometric inverse square law.

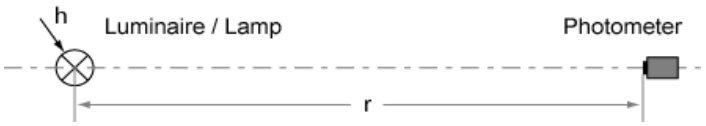

$$E_v = \frac{I_v}{r^2}.$$

This relation holds true only for a point light source, i.e., in the case of large light sources, the luminous intensity calculated by means of this method is faulty [17]. The size of the error depends on the measuring distance and the size, structure and radiation characteristic of the light source. In the standards pertaining to the respective DUT classes, so-called limiting photometric distances are defined in the case of which the error is below an acceptable order of magnitude [18]. Common measuring distances for the measurement of luminaires range from 10 to 30 m.

For measuring the luminous intensity distribution according to this measuring procedure, goniophotometers are employed which capture the illumination intensity at a sufficiently large measuring distance and in all radiation directions. Here, the following options are available:

1. The DUT is moved around two axes and directed towards the detector (turning luminaire goniophotometer)
2. Moving mirror goniophotometer (DUT is moved only around vertical axis)
3. Detector is moved around the DUT (practicable only for short measuring distances)

5.2 Near-field measurement via the integration of luminances

Alternatively to the measurement of luminous intensities via the illuminance, there is another method available: the integration of luminances, which is also mentioned in the standard CIE 70-1987 [19]. As a further development of the procedures described here, in 1991 the TechnoTeam company got a patent for a camera-based measuring principle for luminance integration [2]. This measuring principle is based on the measurement of ray data and the transformation to the luminous intensity distribution (cf. paragraph 4.2). Later, the same measuring principle got a patent in the USA [3].

The near-field goniophotometers based on this measuring principle offer a number of advantages over the classical far-field goniophotometers:

- short measuring distance and, thus, compact measuring systems also suitable for smaller rooms
- The limiting photometric distance does not have to be taken into consideration.

- The measurement of the luminous intensity distribution is independent of the photometric center of the DUT.
- less sensitive to scattered light from the surroundings
- The ray data can also be used for near-field calculations.
- luminance images for more complex measurement tasks (e.g. glare evaluation)

5.3 Indirect measurement via measuring wall

Particularly for measuring headlamps and similar products, the indirect measurement of the LID via a projection wall has become established. Here, the luminance distribution is captured on a measuring wall in a highly resolved way - by means of a luminance measuring camera – beyond the limiting photometric distance. Afterwards, provided that there is an ideal diffuse reflection condition (Lambert reflection), it can be calculated into the illuminance distribution and finally into the luminous intensity distribution.

This measuring procedure offers the essential advantage of an extremely short measuring time over the classical far-field goniophotometers. This is very important particularly for the measurement of modern headlamps with many electronically controllable distributions (LED Matrix headlamps). The TechnoTeam company has specialized in the optimization of the scattered light in this measuring procedure, and offers systems which can be employed in the place of far-field goniophotometers or which can be combined with them [20].

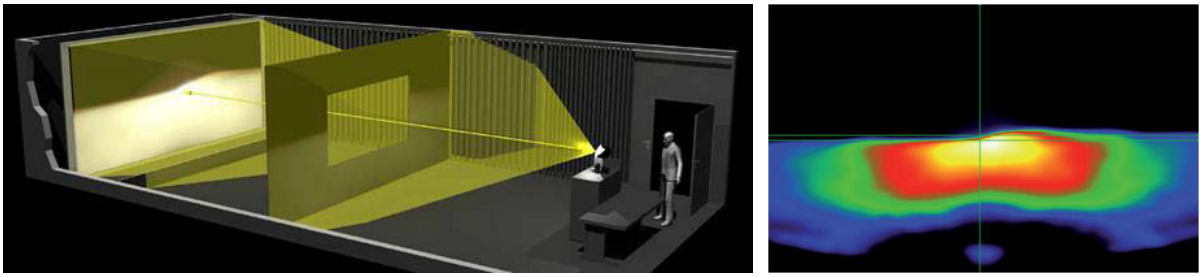

Figure 19: Measurement room for indirect headlamp measurements (left) and LID (right)

5.4 Conformity with IES LM-79-08 and CIE S 025

For the measurement of SSL light sources, the current standards IES LM-79-08 [21] and CIE S 025 [18] (identical with EN 13032-4 [22]) should be taken into consideration. In these standards, the requirements to be fulfilled by the goniophotometers are laid down, but these requirements are not met by all systems or also they require additional expense for the measurements. The essential requirement fixed by the LM-79-08 standard is a type C goniometer (LM-75-01 [23]). Anyway, it is not the C coordinate system which is meant here, but the axis arrangement and moving pattern of the goniometer. Those moving detector and moving mirror goniophotometers are allowed in the case of which the luminaire position is kept unchanged with respect to gravity, that is, no turning luminaire goniophotometers. Although the CIE S 025 standard permits also other types of goniophotometers, it must be guaranteed in this case that the effects on the operating conditions of the luminaire are detected and corrected if necessary.

The near-field goniophotometers type RiGO801 made by the TechnoTeam company are in conformity with both standards. These systems represent type C goniometers in the case of which the sensors (measuring camera and photometer) are moved around the stationary DUT. The luminous flux is measured according to the measuring principle of the integration of illuminances (CIE 84: 1989 [24]). The underlying measurement procedure of the luminance

integration is mentioned in the standard CIE 70-1987 [19] to which finally all standards for the measurement of luminous intensities refer (CIE S 025, LM-79-09 → LM-46-04 / LM-41-98 / LM-20-94 / LM-75-01 → CIE121-1996 → CIE 70.1987).

6. ASPECTS OF GLARE EVALUATION

The subject of the glare evaluation is extremely complex. Due to the physiological and psychological aspects of human vision it can be handled mathematically and metrologically only for certain boundary conditions.

Many glare values are based on the luminous flux coming into the eye, i. e. the illuminance at the eye. This results from the luminance of the source of the glare L_s and the solid angle Ω under which it is seen. Studies have shown that this "simple" approach is not sufficient. The brightness distribution of the light sources is also crucial for the glare impression. For this reason, glare evaluations were developed in which, in addition to the illuminance at the eye, the luminance distribution is taken into account. The Unified Glare Rating (UGR) was developed to unify the various methods and was presented in 1995 [25].

$$UGR = 8 \cdot lg\left[\frac{0{,}25}{L_b}\sum\frac{L_s^2\Omega}{P^2}\right]$$

With

UGR	Unified Glare Rating, glare index
L_b	Background luminance (cd/m²)
L_s	Mean luminance of the single light source in observer direction (cd/m²)
Ω	Solid angle of the light source from observer direction (sr)
P	Position index according to [26]

This method is easy to handle with simple luminaire geometries and uniform luminance distributions of the light source and the background. The necessary data can be obtained from the luminous intensity distribution of the luminaires by assuming a mean luminance for the luminous area. This simple approach can no longer be used for very small and structured light sources. In particular this is because of the square proportion of the luminance which gets a large influence in case of small areas with high luminances, as often occur with SSL products.

This means that the real spatial resolved luminance distributions of the glare sources are significant for the glare impression. An expansion of the UGR method with regard to these problematic light sources was made in [27].

By means of image-resolving luminance measurement technology, a more realistic glare evaluation can take place. However, the development of uniform standardized procedures is necessary. Further sources of literature on this topic can be found, for example, in [28] and [29].

REFERENCES

[1] S. Wendel, Freiform-Optiken im Nahfeld von LEDs, Karlsruher Institut für Technologie (KIT), KIT Scientific Publishing, 2014.

[2] R. Poschmann, M. Riemann and F. Schmidt, "Verfahren und Anordnung zur Messung der Lichtstärkeverteilung von Leuchten und Lampen". DE Patent 41 10 574, 30 March 1991.

[3] I. Ashdown, "Near-Field Photometric Method and Apparatus". USA Patent 5,253,036, 12 October 1993.

[4] V. Jacobs, R. R. W. Van Gaever, M. Diltour, J. Audenaert, B. Van Giel, P. Hanselaer and P. Rombauts, " Simulating surgical luminaires by ray files," *Proceedings of the 5th International Conference on Optical Measurement Techniques,* pp. 175-183, 2012.

[5] M. Landy and J. A. Movshon, "The Plenoptic Function and the Elements of Early Vision," *Computational Models of Visual Processing, Cambridge, MA: MIT Press,* pp. 3-20, 1991.

[6] Wikipedia, "Light field," [Online]. Available: https://en.wikipedia.org/wiki/Light_field.

[7] TechnoTeam Bildverarbeitung GmbH, "Goniophotometer," [Online]. Available: http://www.technoteam.de/product_overview/goniophotometer/index_eng.html.

[8] TechnoTeam Bildverarbeitung GmbH, "Imaging luminance and color measuring devices," [Online]. Available: http://www.technoteam.de/product_overview/lmk/index_eng.html.

[9] TechnoTeam Bildverarbeitung GmbH, "Converter801 - Generating ray files," [Online]. Available: http://www.technoteam.de/product_overview/goniophotometer/software/converter_801/index_eng.html.

[10] V. Jacobs, J. Audenaert, J. Bleumers, G. Durinck, P. Rombauts and P. Hanselaer, "Rayfiles including spectral and colorimetric information," *Optics Express,* pp. 2240-2251, vol.23 (3) 2015.

[11] I. Rotscholl, K. Trampert, U. Krüger, M. Perner, F. Schmidt and C. Neumann, "Determination of tailored filter sets to create rayfiles including spatial and angular resolved spectral information," *Optics Express,* November 2015.

[12] IES TM-25-13 , "Ray File Format for the Description of the Emission Property of Light Sources," Illuminating Engineering Society, 2013.

[13] F. Gaßmann, U. Krüger and T. S. F. Bergen, "Comparison of luminous intensity distributions," *Lighting Research & Technology,* vol. 49, pp. 62-83, 2015.

[14] Wikipedia, "Nyquist–Shannon sampling theorem," [Online]. Available: https://en.wikipedia.org/wiki/Nyquist%E2%80%93Shannon_sampling_theorem.

[15] Wikipedia, "Multidimensional sampling," [Online]. Available: https://en.wikipedia.org/wiki/Multidimensional_sampling.

[16] Wikipedia, "Optical flow," [Online]. Available: https://en.wikipedia.org/wiki/Optical_flow.

[17] V. Jacobs, P. Blattner, Y. Ohno, A. Bergen, U. Krüger, P. Hanselaer, P. Rombauts and F. Schmidt, "ANALYSES OF ERRORS ASSOCIATED WITH PHOTOMETRIC DISTANCE IN GONIOPHOTOMETRY," *Proc., the 28the Session of CIE,* pp. 458 - 468, June 29-July 3, 2015.

[18] CIE S 025:2015, "Test Method for LED Lamps, LED Luminaires and LED Modules," CIE, 2015.

[19] CIE 070-1987, "The Measurement of Absolute Luminous Intensity Distributions," CIE, 1987.

[20] C. Schwanengel, F. Schmidt, T. Reiners and C. Diem, "Das Beste aus zwei Welten – Kombination von Goniophotometrie und digitaler Bildverarbeitung - The best of two worlds – Combining goniophotometry and digital image processing," *Proceedings LICHT 2016, Karlsruhe, 25. – 28. September,* 2016.

[21] IES LM-79-08, "Approved Method: Electrical and Photometric Measurements of Solid-State Lighting Products," Illuminating Engineering Society, 2008.

[22] EN 13032-4:2015-08, " Light and lighting - Measurement and presentation of photometric data of lamps and luminaires - Part 4: LED lamps, modules and luminaires," 2015.

[23] IES LM-75-01, "Goniophotometer Types and Photometric Coordinates," 2001.

[24] CIE 84:1989, "The measurement of luminous flux," 1989.

[25] Technical Report CIE 117, "Discomfort Glare in Interior Lighting," CIE, Vienna, 1995.

[26] M. Luckiesh and S. K. Guth, "Brightness in the visual field and the border of comfort and discomfort (BCD)," *Illuminating Engineering,* no. 44, pp. 650-670, 1949.

[27] CIE 147, "Glare from Small, Large and Complex Sources," CIE, Vienna, 2002.

[28] C. Funke and C. Schierz, "EXTENSION OF THE UNIFIED GLARE RATING FORMULA FOR NON-UNIFORM LED LUMINAIRES," Lux junior, 2015.

[29] T. Porsch, F. Schmidt, C. Funke and C. Schierz, "Ist eine objektive Beschreibung der Störempfindung bei künstlicher Beleuchtung möglich?," *LICHT,* no. 7/8 2015, pp. 70-74.

[30] CIE 121-1996, "THE PHOTOMETRY AND GONIOPHOTOMETRY OF LUMINAIRES," CIE, 1996.

CONTACTS

Knut Bredemeier knut.bredemeier@technoteam.de